J Pathol Inform

Editor-in-Chief:
Anil V. Parwani , Pittsburgh, PA, USA
Liron Pantanowitz, Pittsburgh, PA, USA

OPEN ACCESS
HTML format

For entire Editorial Board visit : www.jpathinformatics.org/editorialboard.asp

Original Article

Application of whole slide image markup and annotation for pathologist knowledge capture

Walter S. Campbell, Kirk W. Foster, Steven H. Hinrichs

Department of Pathology and Microbiology, University of Nebraska Medical Center, Omaha, USA

E-mail: *Walter S. Campbell - wcampbel@unmc.edu
*Corresponding author

Received: 07 May 12 Accepted: 11 January 13 Published: 28 February 2013

This article may be cited as:
Campbell WS, Foster KW, Hinrichs SH. Application of whole slide image markup and annotation for pathologist knowledge capture. J Pathol Inform 2013;4:2.

Available FREE in open access from: http://www.jpathinformatics.org/text.asp?2013/4/1/2/107953

Abstract

Objective: The ability to transfer image markup and annotation data from one scanned image of a slide to a newly acquired image of the same slide within a single vendor platform was investigated. The goal was to study the ability to use image markup and annotation data files as a mechanism to capture and retain pathologist knowledge without retaining the entire whole slide image (WSI) file. **Methods:** Accepted mathematical principles were investigated as a method to overcome variations in scans of the same glass slide and to accurately associate image markup and annotation data across different WSI of the same glass slide. Trilateration was used to link fixed points within the image and slide to the placement of markups and annotations of the image in a metadata file. **Results:** Variation in markup and annotation placement between WSI of the same glass slide was reduced from over 80 μ to less than 4 μ in the x-axis and from 17 μ to 6 μ in the y-axis ($P < 0.025$). **Conclusion:** This methodology allows for the creation of a highly reproducible image library of histopathology images and interpretations for educational and research use.

Key words: Data storage, digital pathology, knowledge management, whole slide imaging

Access this article online

Website: www.jpathinformatics.org

DOI: 10.4103/2153-3539.107953

Quick Response Code:

INTRODUCTION

The process of creating high-resolution digital images of histologic material is gaining acceptance in the pathology community for many uses including training,[1-4] remote consultation,[5-8] and clinical review.[9,10] Whole Slide Imaging (WSI) is U.S. Food and Drug Administration (FDA)-approved for diagnostic use in quantification of breast cancer markers including estrogen receptor quotient, progesterone receptor quotient, and human epidermal growth factor receptor 2 (HER 2/NEU).[11] Evidence of WSI as a reliable primary diagnostic tool in surgical pathology is building with several recent studies showing accuracy equivalent to direct viewing with a light microscope.[7,12-18]

Whole Slide Imaging technology affords its users the ability to view and markup (i.e. outline) areas of diagnostic interest. These areas of interest (AOI) can be further annotated by the pathologist to record diagnostic comments and conclusions based on the interpretation of each AOI. In current pathology practice, significant diagnostic findings identified by the pathologist may be communicated by the placement of an ink mark on the glass slide in the approximate area of the critical diagnostic feature. The ink mark can be used by one pathologist to convey to another the location of the area of interest on the glass slide. Should the ink mark be removed or a notation about its significance not be included in the associated report, the information conveyed by the ink mark is lost. While data contained

within the pathology report may indicate the specific slide or diagnostic AOI containing particularly notable findings, in most situations today, there is no automated linkage between the slide AOI and the pathologist's interpretation embedded within the report. The pathology report contains the sum total of the pathologist's interpretation of the histologic features present within the tissue specimen but may not contain a full discussion of each finding in the slide that resulted in the overall conclusion. Linking pathologist interpretation and thought processes with the actual visual information as an expression of pathologist knowledge would yield critical information. The opportunity to capture and build upon accumulated knowledge would enhance the educational process and invite new approaches to translational research.

Image markup and annotation data recorded during WSI examination represents an improvement to an ink mark on a glass slide for purposes of communicating information between pathologists, but image markup and annotation data do have limitations. According to the Digital imaging and communications in medicine (DICOM) WSI standard,[19] the frame of reference refers to the Cartesian coordinates for all image features and annotations. It "typically only applies to a single mounting of a slide on a particular microscope stage; there is no guarantee that a subsequent mounting of the slide, even on the same equipment, will allow reproducible positioning to the exact same location."[19] As a result, transferring image markup and annotation data across images of the same histopathology slide by means of the DICOM frame of reference may prove difficult. One alternative is to establish a numbering system for each pixel on the scanned image and each pixel of the image markup in relation to the Image Matrix (IM), which is the area scanned, and fixed reference points within the IM. Markup and annotation data can be retained in a pixel-to-pixel relationship apart from the DICOM frame of reference.

The goal of this study was to establish a process for reliably linking WSI data with the pathologist's decision-making process without requiring long-term storage of the entire WSI file. This latter issue was important since long term WSI data storage can consume large amounts of costly storage space.[20-22] It was hypothesized that image markup and annotation data created within a WSI can be associated with a newly acquired WSI of the same glass slide to accurately identify and retain the diagnostic features and interpretations of the diagnosing pathologist. Further, it was hypothesized that accurate restoration of image metadata was possible using existing mathematical principles. This research investigated a method to accurately transfer image markup and annotation data across images of the same histopathology slide scanned at different points in time using pixel-to-pixel association.

METHODS

Basic geographic concepts and distance measurement features of the histopathology slide including WSI image markup and annotation were defined. The definitions used by the DICOM WSI standard in two dimensions were employed for purposes of consistent nomenclature wherever possible. The DICOM WSI standard defines the layout of the histopathology slide as shown in Figure 1. The slides in this study were oriented with the label at the top, and used the Cartesian coordinate system with two dimensions: X and Y, to establish the DICOM frame of reference.

A computational method for designating specific locations on a slide was identified from the literature and is hereafter referred to as trilateration.[23] In brief, the trilateration method uses spherical geometry in three dimensions or circular geometry in two dimensions to locate a point in space in relation to specified reference points when only the distances of the point in space

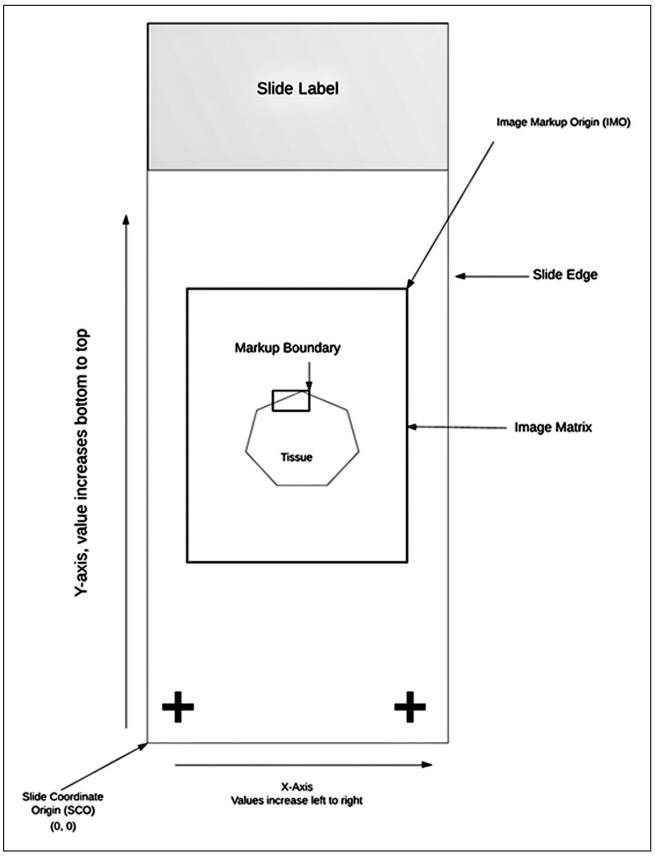

Figure 1: Digital imaging and communications in medicine (DICOM) histopathology frame of reference. With the slide in a vertical orientation and label at the top of the slide, the lower left-hand corner of the slide was designated the Slide Coordinate Origin (SCO) with x, y coordinate values of (0, 0). X-axis values increase from left to right, and y-axis values increase from bottom to top. The region of the slide scanned was defined according to DICOM as the Image Matrix (IM). The top right-hand corner of the IM was defined as the Image Matrix Origin (IMO). The Cartesian coordinates of the IMO were determined relative to the SCO

to each reference point are known. The concept is similar to triangulation, but trilateration more readily accommodates three dimensions, an important feature when considering z-stacking of WSI. The capability to accurately transfer image annotation and markup data across images was investigated by comparing trilateration with existing approaches. To test the effectiveness of the trilateration computational method, it was necessary to determine the baseline capability of a commercial scanning system. This was accomplished by capturing WSI of histologically prepared material of two types, either renal biopsy tissue or breast biopsy tissue. Cases were selected from the files of the surgical pathology department that contained well-characterized histologic features including 11 slides of renal tissue and five slides of breast biopsy tissue. These slides were scanned using a Ventana iCoreo scanner (Ventana Corporation, Tucson, AZ). Table 1 lists each slide and the corresponding diagnostic feature of interest within the tissue specimen. Each slide was reviewed by a pathologist, and a unique, diagnostic feature was outlined (marked up) by a rectangle. The rectangle was restricted in size, so the specific morphologic feature was localized within the markup boundary [Figure 2a]. The pathologist then annotated the marked-up feature in clinical terms describing the diagnostic feature contained within the markup boundary [Figure 2a].

For the first component of the study, each renal slide was scanned 30 times in *ad hoc* order and placement within the scanner carrousel to account for potential mechanical and glass medium variations. To ensure the consistency of the area captured between scans, the IM was manually set to the maximum device setting (i.e., 105,152 × 48,800 pixels @ 0.465 microns/pixel). The WSI device software defined the top right corner of the scanned IM as the (0, 0) coordinate, the equivalent of the DICOM defined Image Matrix Origin (IMO). The scanner, however, diverts from the DICOM slide coordinate definition by orienting the slide with the label on the left [Figure 3]. X-axis values increase from left to right, and y-axis values increase from top to bottom. This location and numbering system was subsequently used to determine the amount of variation in placement of the IMO between scans.

Image markup and annotation (metadata) files created by the vendor viewing application were saved in extensible markup format (XML) format. Contents of the metadata files consisted of the uniform resource locator (URL) of the actual jp2 formatted image file, general slide annotations, image markup coordinates, and markup-specific annotations. Figure 2b represents an example of the metadata file for the image in Figure 2a. Markup coordinates were based on a Cartesian coordinate system with pixel locations representing the x and y coordinates.

Upon completion of each round of slide scanning, the image markup and annotation files for each of the initial WSI files were exported using vendor-supplied import/export tools and then imported into each of the newly acquired images using the same vendor import/export tool. The vendor export/import tool created a new metadata file with the new URL for the image to which the XML was associated. The x, y coordinates for all markup boundaries were unchanged by the import/export process.

Table 1: Renal morphologies marked up and annotated

Case number	Abnormal morphology
Case 1	Lymphocytic tubulitis
Case 2	Intracapillary fibrin thrombus
Case 3	Mesangiolysis
Case 4	Arteriolar fibrinoid necrosis
Case 5	Acute tubular injury
Case 6	Endotheliitis
Case 7	Arteriolar hyaline
Case 8	Arteriolosclerosis
Case 9	Cellular crescent
Case 10	Isometric vacuolization
Case 11	Interstitial edema

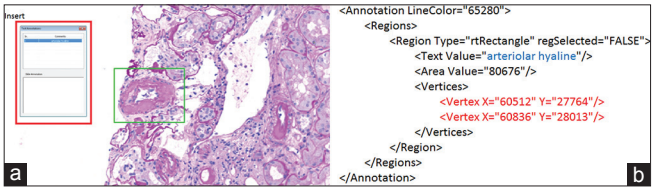

Figure 2: (a) Annotation of diagnostic feature. Markup boundary of arteriolar hyaline structure is shown. Insert shows annotation corresponding to markup (b) Representative portion of Image Metadata for image in Figure 2a. File in XML format. Markup boundary coordinates indicated in red. Physician diagnostic annotation indicated in blue

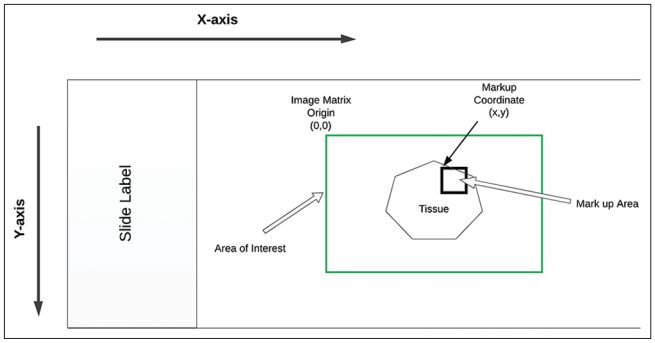

Figure 3: Ventana iCoreo slide frame of reference as applied to study. The ventana slide frame of reference differed from the Digital imaging and communications in medicine histopathology slide frame of reference. Specifically, the slide was placed a horizontal position with the slide label on the left-hand side of the slide. The image matrix origin was set to coordinate (0, 0). X-axis values increased from left to right, and y-axis values increased from top to bottom. No reference was made to the slide coordinate origin

To assess the accuracy of markup placement on each subsequent WSI of the same slide, a specific, readily identifiable tissue landmark (e.g., a small blood vessel or a unique tissue formation) was located within each image and the distance from the landmark to the edges of the markup boundary was measured in the x and y axis. The impact of any possible movement of the IMO was assessed relative to the markup rectangle on the slide. The changes in the markup location to the tissue landmark were calculated including average change and standard deviation of change. Examples of measurements and calculations are detailed in Figures 4a and b.

In the second portion of the study, a novel method to "normalize" differing WSI Frames of Reference and perform a pixel-to-pixel match was developed. The model introduced the use of two cross-hatches etched onto the surface of the glass slide as commonly found on commercially produced histopathology slides [Figure 1]. After scanning, marking-up, and annotating the histopathology slide, distances between the two glass etchings and the markup boundaries were measured and retained. Using the retained dimensions and the geometric principle of trilateration, the precise location of the image markup in relation to the intended architectural features was calculated [Figure 5].

To test the accuracy of the trilateration computational method for association of image markup and annotation metadata files, the computational methods were applied to 30 independent scans of the same glass slide. The original image metadata file was imported to each newly acquired image. The calculated values for each markup location were inserted into the XML metadata file. The images with modified metadata files were then viewed and the distances of the markup boundary to the intended tissue feature was measured in the x and y axis. The average change in location and the standard deviation of markup location changes were calculated as noted previously in Figure 4. The *F*-test statistic was used to compare the difference in standard deviation of markup location between methods of markup placement, that is by the computational method and without use of the computational method.

The third component of the study focused on the ability of the trilateration process to relocate multiple markup and annotation data of multiple diagnostic features within the same slide. Five representative slides from two breast biopsy cases, one malignant and one benign, were scanned, marked-up, and annotated. Table 2 details the slides and diagnostic features marked-up and annotated within each image. Each slide was then scanned for comparison purposes for an additional three times. Image metadata files were exported from the initial image file and imported to the newly acquired image files. Coordinates for each markup boundary were calculated using the proposed technique, and the calculated coordinate values were inserted into the XML metadata file for each image. The positional change for each markup boundary to the intended tissue features was measured and compared to the original markup location. Variation in markup locations within the breast biopsy cases was then compared to the variation in the renal cases using the *F*-test statistic.

Table 2: Abnormal breast morphologies marked up and annotated by slide

Slide	Abnormal morphologies
Slide 1	Two areas of ductal carcinoma *in situ* (DCIS); two areas of DCIS suspicious for invasion
Slide 2	DCIS with possible invasion using immunohistochemistry stains (AE1/AE3)
Slide 3	DCIS with possible invasion using additional immunohistochemistry stains (p63)
Slide 4	Apocrine change
Slide 5	Two areas of florid usual hyperplasia; one area of elastosis; and one area of adenosis

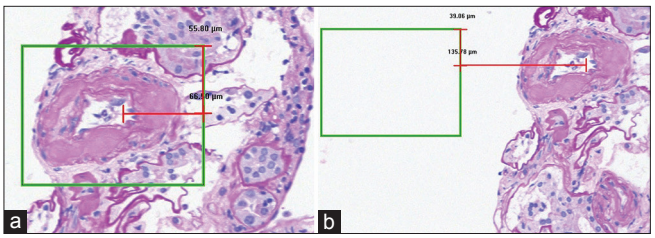

Figure 4: (a) Markup of arteriolar hyaline structure and measurements of outline boundaries to tissue feature within tissue morphology. (Measurements in red) (b) Placement of original markup of arteriolar hyaline structure in newly scanned image of the same slide with measurements of outline boundaries relative to the same tissue feature

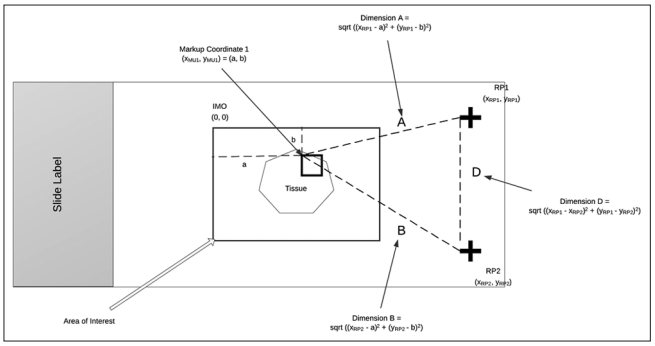

Figure 5: Trilateration dimensions and formulas using the ventana slide frame of reference. The frame of reference was normalized by using two reference points. Distances for dimensions A, B, and D were known from the original scan. New values for markup coordinates in subsequent scans were determined using the above equations and the coordinates of the reference points based on the new scan frame of reference

RESULTS

Vendor image markup and annotation tools were employed to annotate histology slides scanned at ×20 from two different organ systems including kidney and breast. The accuracy of the vendor-supplied markup and annotation placement tools and their ability to relocate the same diagnostic feature in a newly acquired image of the same glass slide was assessed. After comparing the original metadata file with the newly created image file, the variation in location of the image markup AOI's ranged from 120 μ to 407 μ in x-axis and 64-310 μ in the y-axis. The standard deviation of markup location change in relation to the specified tissue landmark within each image ranged from 82.18-322.18 μ in the x-axis to 17.34-112.34 μ in the y-axis [Table 3]. In terms of renal histology, this variation represented between 2 and 3 times the width of a glomerulus at the vascular pole, the widest portion of the glomerulus. In practice, the intended target shifted between 1/3 and 1/2 of a light microscope 20 × field of view.

The trilateration method, with an embedded reference point, demonstrated a reduced variation in markup location placement. The standard deviation of markup location change in relation to the specified tissue landmark within the image was 9.85 μ in the x-axis and 11.02 μ in the y-axis. This represented both substantial and significant reduction in location placement variation as measured by the F-statistic ($F_{x\text{-axis}} = 106.18$; $F_{y\text{-axis}} = 7.47$; $F_{critical} = 2.495$; $P < 0.025$)[24] [Table 4].

The ability of the trilateration method to relocate multiple morphologic features was also assessed. The original image markup and annotation metadata files were imported using calculated markup coordinates to locate the markup boundaries and markup location to multiple specific tissue landmarks. It was found that for each case, the intended diagnostic feature was contained within the markup boundaries. The standard deviation of markup location change was 3.79 μ in the x-axis and 5.84 μ in the y-axis. These results for location placement variation using vendor tools were compared to the trilateration method for markup placement as measured by the F-statistic and were determined to be significant and substantial. ($F_{x\text{-axis}} = 694.07$; $F_{y\text{-axis}} = 29.52$; $F_{critical} = 2.008$; $P < 0.025$).[24] Calculations are found in Table 5.

Table 3: Standard deviation in distances from tissue landmark to markup boundaries using vendor tools to associate markup files with image files

Case	Scans	σ x-axis (μ)	σ y-axis (μ)
1	29	94.98	18.83
2	29	159.01	25.01
3	29	250.18	112.34
4	30	150.86	24.23
5	30	159.17	18.04
6	24	322.18	26.47
7	30	99.85	31.73
8	30	85.85	23.19
9	30	239.38	18.88
10	30	82.18	17.34
11	30	117.93	20

Table 4: Comparison of standard deviation in distances from tissue landmark to markup boundaries when using computational methods versus vendor tool alone

Description	Computation method
Case	7
No. of scans	30
σ x-axis (μ)	9.69
σ y-axis (μ)	11.61
Degrees of freedom (numerator)	29
Degrees of freedom (denominator)	29
F value (x-axis)	106.18
F value (y-axis)	7.47
F-critical (*P*<0.025)	2.495

Table 5: Comparison of standard deviation in distances from tissue landmark to markup boundaries when using computational methods for breast biopsy slides versus vendor tool alone

Description	Vendor tools only	Computation method
Case	7	7
No. of scans	30	36
σ x-axis (μ)	99.85	3.79
σ y-axis (μ)	31.73	5.84
Degrees of freedom (numerator)	29	
Degrees of freedom (denominator)	35	
F value (x-axis)	694.07	
F value (y-axis)	29.52	
F-critical (*P*<0.025)	2.008	

DISCUSSION

This study investigated the accuracy of image markup metadata files to be placed onto newly acquired images and thereby convey the diagnostic features identified by the pathologist during review of the original WSI of the glass slide. The native tools embedded within the WSI scanning device and viewing software were capable of annotation but could not sufficiently relocate the area of interest when the slide was rescanned at a later date to a high degree of accuracy. For example, if the morphologic feature exceeded was small (<100 μ), it

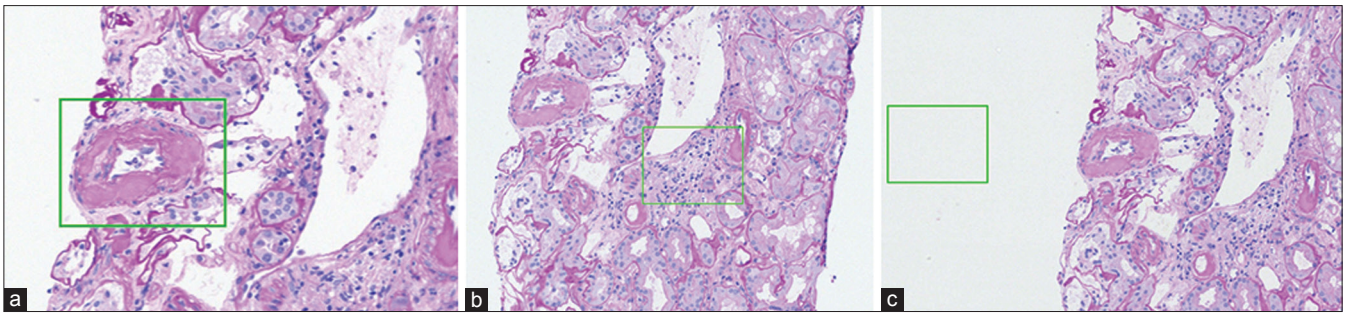

Figure 6: (a) Example of markup placement variation between newly scanned images of the same slide. A–Accurate markup placement indicating arteriolar hyaline structure (b) Markup placed onto renal tissue incorrectly indicating arteriolar hyaline morphology (c) Example of markup intended to indicate arteriolar hyaline structure placed outside of tissue image

was not accurately relocated in newly scanned images of the same slide. Although the width of the biopsy core was ≤1 mm, in some instances, no tissue was contained within the markup boundary [Figures 6a-c]. The cause for this phenomenon was explored and is believed to be based in the establishment of the frame of reference and coordinate system used by the scanner. The relative location of the IMO changed in relation to the location of the tissue each time the slide was scanned. This was concluded to be due to movement of the slide in the holder or a related mechanical process variation [Figure 7].

The computational method employed in this study used two cross-hatch etchings on the glass slide as reference points with which to trilaterate and calculate the precise location of the image markup boundaries. Since the etchings on the glass slide maintained their spatial relationship with the tissue, they could serve as reliable geographical reference points to use in trilateration calculations. This approach addressed the challenge of compensating for mechanical shifting of the slide during placement or selection from the carousel. The computational method was equally effective for slides with multiple marked-up diagnostic features or for a single diagnostic feature.

The results support the hypothesis that image markup and annotation data can be created with a particular WSI device and accurately transferred to newly created images of the same slide using the proposed computational methods. The impact of this finding is that a WSI can be examined by a pathologist and the significant diagnostic features identified during examination can be captured, retained, and if necessary, put back into their original context, thereby permitting the elimination of the large WSI files without loss of data. The method could be enhanced in the future without the need for excessive data storage requirements by storing only the portion of the image contained within the markup boundaries. In this way, an image library of histopathology images and their corresponding interpretations could be developed.

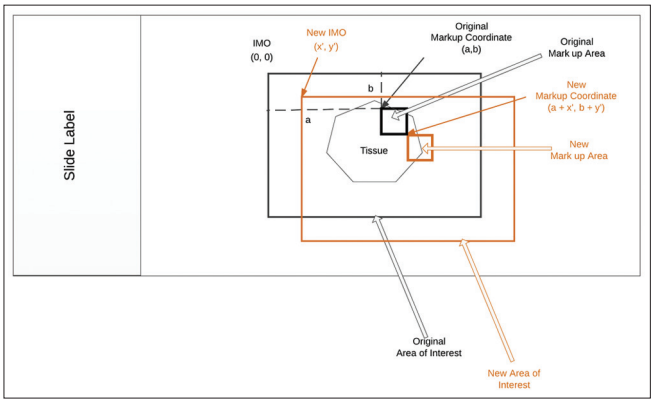

Figure 7: Effect of Image Matrix Origin location relative to tissue specimen on the placement of the image markup

Using this approach, pathology report enhancement can be achieved through the integration of the WSI viewing software and the laboratory information system. Diagnostic features identified by the examining pathologist can be specifically referenced within the microscopic section of the pathology report to indicate the precise slide and location of each tissue morphology used to reach a definitive diagnosis. If desired, images of diagnostic importance could also be imported to the microscopic exam section of the report. Using standardized encoding of annotations (e.g., standardized nomenclature of medicine clinical terms, that is, SNOMED-CT expressions), information captured during microscopic examination could be mapped onto data elements synoptic reports and disease registries to automate pathologist administrative tasks and improve efficiency.

For the pathologist in training, an encoded pathology image repository could be used to present numerous examples of tissue morphologies representative of a given disease. Assuming a large set of images, it is possible to increase the trainee's exposure to a broader representation of disease expression *in silica* than can be afforded *in vivo* by any one residency program. It is also possible to create training and testing scenarios using the stored images to challenge the resident with achieving accurate

differential diagnoses given mock-up case scenarios and presentations.

An interesting byproduct of the findings of this study is the potential impact on WSI data storage costs. Long-term storage costs of WSI files are large due to the large size of WSI data files. Assuming the longevity and integrity of the glass slide overtime, the concepts may provide for alternative methods of managing WSI files where only the diagnostically important features of the image are retained digitally. This would result in a reduction of data storage requirement for WSI and potentially improve the value-added approach for WSI.[21]

All tests in this study involved a single WSI device and single vendor. Other devices and vendors employ a variety of methods of image capture, image registration, and microscope stage mechanisms. The geometric principles used for the computational approach apply regardless of platform but, in the absence of an image management standard, they would need to be adjusted for each WSI platform. In the future, the approaches used in this study could be used to link morphologic observations with standardized terminology to improve retention and usage of pathologist knowledge in education and genomic research.[25,26]

ACKNOWLEDGMENTS

We thank James Campbell, MD, James McClay, MD and Thomas Lane, PhD for helpful comments and discussion.

REFERENCES

1. Foster K. Medical education in the digital age: Digital whole slide imaging as an e-learning tool. J Pathol Inform 2010; 1. pii: 14.
2. Giansanti D, Castrichella L, Giovagnoli MR. The design of a health technology assessment system in telepathology. Telemed J E Health 2008;14:570-5.
3. Bruch LA, De Young BR, Kreiter CD, Haugen TH, Leaven TC, Dee FR. Competency assessment of residents in surgical pathology using virtual microscopy. Hum Pathol 2009;40:1122-8.
4. Zwönitzer R, Hofmann H, Roessner A, Kalinski T. Virtual 3D microscopy in pathology education. Hum Pathol 2010;41:457-8.
5. Al Habeeb A, Evans A, Ghazarian D. Virtual microscopy using whole-slide imaging as an enabler for teledermatopathology: A paired consultant validation study. J Pathol Inform 2012;3:2.
6. Wilbur DC, Madi K, Colvin RB, Duncan LM, Faquin WC, Ferry JA, *et al*. Whole-slide imaging digital pathology as a platform for teleconsultation: A pilot study using paired subspecialist correlations. Arch Pathol Lab Med 2009;133:1949-53.
7. Evans AJ, Chetty R, Clarke BA, Croul S, Ghazarian DM, Kiehl TR, *et al*. Primary frozen section diagnosis by robotic microscopy and virtual slide telepathology: The University Health Network experience. Hum Pathol 2009;40:1070-81.
8. López AM, Graham AR, Barker GP, Richter LC, Krupinski EA, Lian F, *et al*. Virtual slide telepathology enables an innovative telehealth rapid breast care clinic. Hum Pathol 2009;40:1082-91.
9. Graham AR, Bhattacharyya AK, Scott KM, Lian F, Grasso LL, Richter LC, *et al*. Virtual slide telepathology for an academic teaching hospital surgical pathology quality assurance program. Hum Pathol 2009;40:1129-36.
10. Ho J, Parwani AV, Jukic DM, Yagi Y, Anthony L, Gilbertson JR. Use of whole slide imaging in surgical pathology quality assurance: Design and pilot validation studies. Hum Pathol 2006;37:322-31.
11. U. S. food and drug administration-recently approved devices. Silver Springs, MD: US Food and Drug Administration; 2012 Available from: http://www.fda.gov/MedicalDevices/ProductsandMedicalProcedures/DeviceApprovalsandClearances/Recently-ApprovedDevices/default.htm. [Last cited on 2012 Apr 16].
12. Al-Janabi S, Huisman A, Vink A, Leguit RJ, Offerhaus GJ, ten Kate FJ, *et al*. Whole slide images for primary diagnostics of gastrointestinal tract pathology: A feasibility study. Hum Pathol 2012;43:702-7.
13. Jukić DM, Drogowski LM, Martina J, Parwani AV. Clinical examination and validation of primary diagnosis in anatomic pathology using whole slide digital images. Arch Pathol Lab Med 2011;135:372-8.
14. Rodriguez-Urrego PA, Cronin AM, Al-Ahmadie HA, Gopalan A, Tickoo SK, Reuter VE, *et al*. Interobserver and intraobserver reproducibility in digital and routine microscopic assessment of prostate needle biopsies. Hum Pathol 2011;42:68-74.
15. Campbell WS, Lele SM, West WW, Lazenby AJ, Smith LM, Hinrichs SH. Concordance between whole-slide imaging and light microscopy for routine surgical pathology. Hum Pathol 2012;43:1739-44.
16. Gilbertson JR, Ho J, Anthony L, Jukic DM, Yagi Y, Parwani AV. Primary histologic diagnosis using automated whole slide imaging: A validation study. BMC Clin Pathol 2006;6:4.
17. Fallon MA, Wilbur DC, Prasad M. Ovarian frozen section diagnosis: Use of whole-slide imaging shows excellent correlation between virtual slide and original interpretations in a large series of cases. Arch Pathol Lab Med 2010;134:1020-3.
18. Koch LH, Lampros JN, Delong LK, Chen SC, Woosley JT, Hood AF. Randomized comparison of virtual microscopy and traditional glass microscopy in diagnostic accuracy among dermatology and pathology residents. Hum Pathol 2009;40:662-7.
19. DICOM Standards Committee, Working Groups 26, Pathology. Digital imaging and communications in medicine (DICOM) Supplement 145: Whole slide microscopic image IOD and SOP classes. Rosslyn, Virginia: Digital Imaging and Communications in Medicine (DICOM); 2010.
20. Hedvat CV. Digital microscopy: Past, present, and future. Arch Pathol Lab Med 2010;134:1666-70.
21. Isaacs M, Lennerz JK, Yates S, Clermont W, Rossi J, Pfeifer JD. Implementation of whole slide imaging in surgical pathology: A value added approach. J Pathol Inform 2011;2:39.
22. Pantanowitz L, Valenstein PN, Evans AJ, Kaplan KJ, Pfeifer JD, Wilbur DC, *et al*. Review of the current state of whole slide imaging in pathology. J Pathol Inform. 2011;2:36.
23. Nature of geographic information-trilateration. University Park, PA: The Penn State University; 2012. Available from: https://www.e-education.psu.edu/natureofgeoinfo/c5_p12.html. [Last cited on 2012 Apr 25].
24. NIST/SEMATECH e-handbook of statistical methods: *F*-test for equality of two variances. Washington, DC: National Institutes of Standards and Technology; 2012. Available from: http://www.itl.nist.gov/div898/handbook/eda/section3/eda359.htm. [Last cited on 2012 Apr 25].
25. Cooper LA, Kong J, Wang F, Kurc T, Moreno CS, Brat DJ, *et al*. Morphological signatures and genomic correlates in glioblastoma. Proc IEEE Int Symp Biomed Imaging 2011;30:1624-7.
26. Cooper LA, Kong J, Gutman DA, Wang F, Gao J, Appin C, *et al*. Integrated morphologic analysis for the identification and characterization of disease subtypes. J Am Med Inform Assoc 2012;19:317-23.